Chapter 1

Introduction

In May 1962, Theodore Harold Maiman demonstrated the first laser operation from a solid state ruby laser [1]. In the following months, extensive research took place on stimulated emission and already by November 1962, several groups began reporting on lasing action in semiconductors [2, 3]. Semiconductor based diode lasers have since been improved in terms of manufacturing, output power, beam quality and spectral coherence [4]. They offer lasing emission ranging between the visible and into the long infrared (IR) wavelengths [5]. Due to their compact size, reliability and cheap manufacturing costs, diode lasers have replaced many solid state, chemical and gas lasers.

These advantages have made diode lasers by far the most common laser type, with several million devices being produced every month. Today, semiconductor diode lasers are found in CD players, laser writers, laser pointers and in the bar code readers in the supermarket. In addition, various medical and industrial fields utilizes diode lasers, and still more and more applications are found [6].

1.1 Tunable diode lasers

The emission wavelength of most, if not all laser sources can in principle be changed by different means. In this work however, tunable refer to laser sources with a mechanism for precise control of the emission wavelength while maintaining a narrow spectral linewidth. Tunable diode lasers holds a strong foothold within various applications. Among the main applications is optical telecommunication, where wavelength tuning is one of many methods to increase the bandwidth transmitted through optical fibers [7, 8, 9].

In addition, tunable lasers especially emitting in the near IR are key components within the field of bio-medical optics, including applications such as Fourier domain optical coherence tomography (OCT) [10, 11], absorption spectroscopy [12, 13] and wavelength modulated Raman spectroscopy (WMRS) [14, 15]. Likewise, applications such as trace-gas detection [16], non-linear frequency conversion [17, 18] and terahertz frequency generation [19, 20] all utilize tunable laser sources.

The specific light source requirements and tuning capabilities varies depending on the targeted application. In some applications, say in OCT, wide wavelength tuning at rapid speeds is needed for obtaining high axial resolution scans at high imaging rates. On the other hand, only tens of milliwatts are needed as you do not want to harm the patients retina during imaging.

Other applications require moderate wavelength tuning but with high output powers. This is e.g. the case in differential absorption light detection and ranging (LIDAR) applications [21], where high output powers are needed to get sufficient back scattered photons at the detector. On the other hand, wavelength tuning should only cover on/off resonance absorption peaks and has instead specific linewidth requirements set by the absorption peaks [22].

1.2 Upconversion IR detection

Spectral detection of IR wavelengths is of great technical and scientific interest, due to the important chemical compounds that display unique and strong IR spectral fingerprints [23]. In addition, IR imaging

is a valuable tool to investigate biological samples, such as histological tissue samples and cell cultures [24, 25]. The non-invasive detection can provide chemical specificity without recourse to labels, and is currently used to understand and identify different types of cancer [26].

In this work, the developed light sources are targeted applications within the field of non-linear frequency conversion, in particular upconversion IR detection. Recently, upconversion detection has had a renaissance due to the progress in the field of IR light sources and non-linear materials. The upconversion technique shifts IR signals into the near IR range, where efficient detection can be made with basic Si-based detectors at room temperature [23]. In comparison, direct detection using traditional IR detectors, e.g. HgCdTe detectors, require cryogenic cooling in order to improve the noise performance [27, 28]. Nonetheless, noise remains a major issue in these detectors, as all objects at room temperature have their Black-body radiation in the IR range, including the detector itself.

In the case of upconversion detection, this problem is solved by first converting the IR signals toward shorter wavelengths, before being detected by efficient and low noise detectors. This technique has proven superior noise performance [23, 29], including single-photon detection at room temperature [30, 31]. In addition, IR hyperspectral imagining has been demonstrated with this technique [32, 33] as well as LIADR applications [34, 35].

Upconversion is based on the non-linear process of sum frequency generation (SFG), where the IR signal is mixed with a pump source inside a non-linear crystal. Under phase matching condition, this result in generation of an upconverted signal with the frequency $\nu_{\mathrm{SFG}} = \nu_{\mathrm{signal}} + \nu_{\mathrm{pump}}$ [36], i.e. a signal with a shorter wavelength of

$$\lambda_{\mathrm{SFG}} = \left(\frac{1}{\lambda_{signal}} + \frac{1}{\lambda_{pump}} \right)^{-1} = \frac{\lambda_{\mathrm{signal}} \lambda_{\mathrm{pump}}}{\lambda_{\mathrm{signal}} + \lambda_{\mathrm{pump}}} \ . \tag{1.1}$$

In addition, to upconvert a wide IR spectrum, the angle of incident at the non-linear crystal or the temperature of the crystal can be changed. By doing so, different phase matching conditions are fulfilled providing upconversion of a broad IR spectrum [37]. Alternatively, and as is intended by this work, by tuning the wavelength of the pump source, different phase matching conditions are fulfilled, providing broad IR upconversion enabling spectroscopy and hyperspectral imaging in the IR [32, 33, 38, 39]. This could provide a quicker method of IR sweeping/detection, where the width of the upconverted IR spectrum will be set by the bandwidth of the upconversion process, together with the total tunability of the pump source.

In summary, the wider the pump wavelength tuning the broader an IR signal can be upconverted, thus addressing more IR features. Moreover, as this is a non-linear process and as the IR signals are expected to be of low power, high pump powers are needed to improve the upconversion efficiency.

1.3 Types of tunable diode lasers

Semiconductor based distributed Bragg reflector (DBR) and distributed feedback (DFB) ridge waveguide (RW) lasers can provide diffraction limited beams, moderate wavelength tuning (< 10 nm) and emit output powers below the watt level [40, 41]. Recently, single wavelength broad-ridge waveguide DBR lasers has been demonstrated with a couple of watts of output power [42].

On the contrary, tapered diode lasers with integrated DBR gratings provide multiple watts of diffraction limited output powers [43], however their tuning capabilities have not been demonstrated. This is mainly due to the complicated structure of these devices, including the challenges of astigmatisms and of obtaining single mode operation. One approach combines tapered power amplifiers (TPA)s in external cavity configurations, which can provide both tuning and high output powers [44, 45]. Such a configuration utilizes a grating which is mechanically adjusted to select and tune the emission wavelength.

Recently, demonstration of electrically pumped tunable vertical cavity surface emitting (VCSEL) lasers with a micro-electro-mechanical system (MEMS) has proved more than 50 nm of tuning at 400 kHz sweeping rates, which makes them ideal for OCT applications [46, 47]. The drawback of this type of laser is the low (< 10 mW) output powers which limits their applications.

The described tunable lasers offers some challenges such as the limited tuning range of DBR and especially DFB lasers, and the low output powers of the VCSEL lasers. In addition, many applications requires continuous tuning which is not typically achieved from the GaAs based DBR and DFB lasers.

1.4 Motivation

The motivation of this work is to develop tunable high power laser sources to serve as compact pump sources in upconversion detection systems. These should act as single-pass pump sources, and replace the standard Nd:YVO_4 laser cavities oscillating at 1064 nm that are typically implemented in upconversion systems [23, 35].

The wavelength of the developed diode lasers will be around $\lambda_{\text{pump}} = 976$ nm, chosen so that the upconverted signals will be near the absorption peak of Si-detectors, i.e. $800 - 900$ nm [48]. Although the difference between 1064 nm and 976 nm is not that significant, the shorter pump wavelength will have a major impact, especially when upconverting longer IR signals (> 10 μm). E.g. assuming a signal around 10 μm [49, 50], the chosen pump wavelength will upconvert the signal to a wavelength of $\lambda_{\text{SFG}} = 890$ nm, see eq. (1.1), which is ideal for Si-based detectors. In addition, replacing a cavity with a single-pass system will reduce the complexity and footprint of the upconversion detection modules, and potentially allow hand-held IR detectors.

In addition, having a wavelength tunability of about 23 nm (major result of this work), an IR sweep of about 243 cm^{-1} can be obtained which can cover whole spectrum of rotational vibrational bands [51]. In terms of hyperspectral imaging, the high output power and the specific wavelength ensures efficient detection (with reduced integration time), and the wide wavelength tunability will provide an increased field of view [33].

While continuous wavelength tuning is important in many spectroscopic applications, mode hops can be tolerated in upconversion detection as long as they are below the nanometer range, which is the typical conversion bandwidth. The investigated light sources of this work provide moderate (< 0.5 W) output powers, while the targeted application requires high pump powers. Therefore, these light sources are implemented in miniaturized master oscillator power amplifier (MOPA) configurations, where the MO provides the wavelength tunability and the PA increases the output power.

The target of this work, beside the development and understanding tunable laser devices, is to reach suitable output powers for upconversion application with wide wavelength tuning around 976 nm.

1.5 Project Scope

This thesis describes shortly some of the theory behind tunable diode lasers in chapter 2, followed by a description of the first laser process, including two reference DBR-RW lasers in chapter 3. This work examine two concepts of achieving wide wavelength tunability. The first consider using monolithically combined tunable multi-wavelength DBR-RW lasers to cover a wider tuning range compared to a single tunable DBR-RW laser, see chapter 4 and 5. In this case, thermal wavelength tuning is obtained by embedding micro-heaters on top of the grating sections as described chapter 6. The second concept consider using widely tunable sampled-grating (SG) DBR-RW lasers, which achieve wide wavelength tunability due to their unique grating features, see chapter 7.

Both investigations include the whole "chain" of development, including laser design, device processing, characterization and optimization, all done with regards to the intended MOPA implementation and targeted application. This MOPA implementation is described in chapter 8 where three different MOPA systems are constructed. These systems have different tunable MO lasers, and utilize TPAs to obtain high output powers.

Chapter 9 describes some early-stage upconversion experiments where the developed MOPA systems have been implemented and tested.

Finally, an outlook is given in chapter 10 describing the further development of this work, in particular different strategies to deal with the limits and challenges of achieving wider wavelength tuning, and higher output powers than those obtained in this work.

Chapter 2

Fundamentals of laser diodes

In this chapter, fundamental concepts of semiconductor lasers will be briefly introduced, as required for understanding laser operation, laser gain and wavelength tuning. The reader is here assumed to have a basic understanding of semiconductor physics. These concepts will be used to describe the relevant device characteristics at later chapters. This chapter begins with the concept of optical gain, with focus on semiconductor heterostructures. This is followed by laser threshold, lateral waveguiding and mode spectrum. The presented theory and the figures of this chapter are inspired by the text books [5, 41, 52].

2.1 Optical Gain in Semiconductors

Semiconductor diode lasers are based on energy bands, with the lower band referred to as the valence band and the upper band referred to as the conduction band. These bands are separated by a gap with energy E_g, and for typical III-V compound semiconductors, this gap is in the range of 0.5 to 2.5 eV, depending on the material composition. The photon energy is defined as [5]

$$E_{\text{photon}} = h\nu = \frac{hc}{\lambda} \ , \tag{2.1}$$

where $h = 4.135 \times 10^{-15}$ eV $\cdot$ s is Plancks constant, ν is the frequency of the light and $c = 3 \times 10^8$ m/s is the speed of light in vacuum. The corresponding wavelengths of the aforementioned band gap energies lie in the range between the blue to the near IR [5].

In the absence of an external pump source and at a temperature $T = 0$ K, the valence band of undoped semiconductors is occupied with electrons while the conduction band will be empty. This is reversed by applying an injection current I_{inj} to the semiconductor material, causing an increase in the concentration of electrons in the conduction band and holes in the valence band. This provides generation and recombination between the electron-hole pairs, leading to four basic electronic transitions. These are illustrated in Fig. 2.1 and include:

(a) Spontaneous recombination (photon emission)

(b) Stimulated generation (photon absorption)

(c) Stimulated recombination (coherent photon emission)

(d) Non-radiative recombinations

The open circles in Fig. 2.1 represent unfilled states (holes) and the solid circles represent filled states (electrons).

First, spontaneous recombination of electrons and holes results in the emission of photons of a wavelength equal to the energy difference between the corresponding levels in the conduction and valence bands. This being said, the emitted photons are random in phase and direction. This emission occurs at a spontaneous transition rate of R_{sp} and is utilized in light-emitting diodes (LED)s.

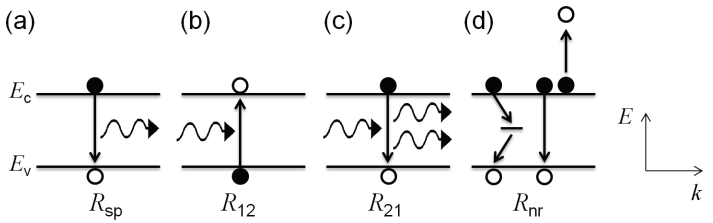

Figure 2.1: *Electronic transitions between the conduction and valence bands showing (a) spontaneous emission (b) photon absorption from level 1 to 2 (c) stimulated emission from level 2 to 1 and (d) two non-radiative recombination processes.*

Photons can also be absorbed by the material which causes generation of new pairs of electrons and holes with a rate of R_{12}, see Fig. 2.1(b). The third transition is stimulated emission, where the generated photons stimulate recombination of additional electrons and holes with a rate of R_{21}. This generation causes simultaneous generation of additional photons that are coherent with the initial photons, in terms of phase and direction, see fig. 2.1(c). This transition is mandatory for laser operation and sets up the two requirements for lasing.

The first requirement is population inversion, i.e. having the number of electrons in the conduction band exceeding the number of holes in the valence band. This is obtained by means of pumping, which in diode lasers is typically done by an electron current. This condition will be discussed further in Sec. 2.4. The second requirement is feedback, which is obtained by positioning the laser medium inside a resonant cavity. By doing so, a number of photons circulate the cavity causing coherent photon emission. In the case of diode lasers, the cavity is typically constructed between coated end facets, with back facets having high reflectivity ($R_b > 90\%$) and the front facet typically having anti-reflection (AR) coating to have high output power. This causes most of the light to be emitted from the front facet where it is typically collected and collimated. Alternatively, and as will be utilized in the next chapters, the back mirror can be made using DBR gratings, which provide high reflectivity in a narrow spectral range leading to a narrow emission linewidth.

The final electron transition is non-radiative, with a rate R_{nr} at which electron-hole pairs are recombined without emission of any photons, through e.g. traps and/or Auger recombination [52], see fig. 2.1(d). This process is unwanted in diode lasers as it reduces the efficiency of the light source and therefore, different design concepts are implemented to reduce these effect.

2.2 Vertical confinement

To fulfill the two laser requirements described in the previous section, diode lasers require a medium providing optical gain, an optical waveguide structure confining photons to the active region and a lateral confinement of photons providing injection current and carriers [5].

Most diode lasers are based on p-i-n double heterostructures consisting of an undoped semiconductor layer embedded between p- and n-doped semiconductors with larger band gaps. More specifically, in this work a graded index separate confinement heterostructure (GRINCH) [53] is used, see Fig. 2.2(a). This structure (GaAs based) has the lowest Al doping level near the active region ($\sim 10^{16}$ cm^{-3}) to reduce absorption effects, while the outer contact and substrate layers have higher doping levels between 10^{18} and 10^{19} cm^{-3} to allow efficient carrier generation and low resistance [54]. A graded doping transition is made between the outer contact and substrate layers and into the active region.

Such structures have the advantage of a narrow carrier confinement (active) region, providing a high recombination rate, separated from the wider graded optical waveguide region, see Fig. 2.2(b). The active region can be realized using single- or multi-quantum well (SQW, MQW). This structure allows optimization of the optical confinement without affecting the carrier confinement. Particularly, smaller band gap semiconductors have higher refractive indices, where the optical field will be confined and

guided, see fig. 2.2(c) and (d). This improved confinement and guiding of a GRINSCH structure provide reduced threshold current and higher output powers [53, 55].

The different vertical structures used in this thesis including the active materials will be described in the next chapters.

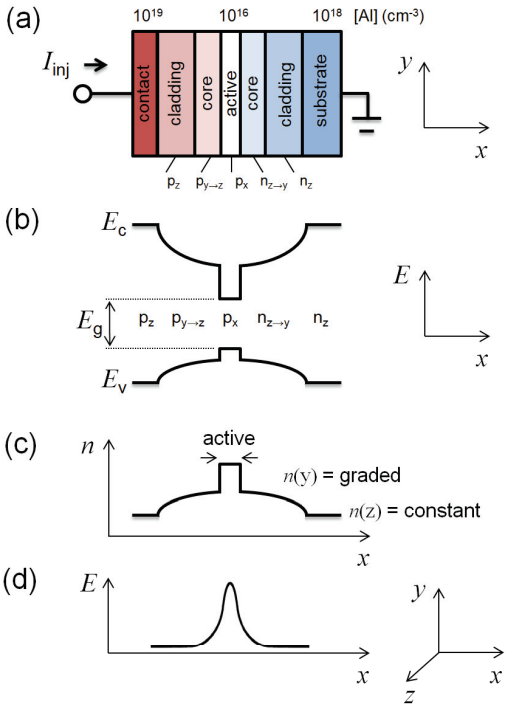

Figure 2.2: *Schematic of the GRINSCH structure showing (a) material structure of the individual layers (b) energy diagram of the conduction E_c and valence E_v band (c) refractive index profile and (d) corresponding electric field profile for a mode travelling in the z-direction.*

2.3 Lateral confinement

Semiconductor diode lasers utilize different concepts for lateral confinement. One concept is gain guiding, which is enabled by defining a current aperture in the contact layer that spatially limits the carrier injection [5]. This means that optical waves outside this aperture will experience high losses, resulting in a lateral confinement of the generated light. This concept is typically used in broad area (BA) lasers where stripe widths of a few hundred microns enable tens of watts of output power [56]. The main disadvantage of BA lasers is the poor beam quality, caused by the high-order lateral modes that can fit within the wide active region [5].

Improved beam quality can be obtained when using narrow stripe width together with the concept of index guiding, which is based on an induced refractive index step in the lateral direction. Similar to an optical fiber, an induced refractive index step provides guiding and confinement in the lateral direction [5].

Assuming a three-layer waveguide (active, core and cladding); the spatial mode characteristics are given by the normalized waveguide thickness D [57]:

$$D = \frac{2\pi d}{\lambda}\sqrt{n_{\text{core}}^2 - n_{\text{cladding}}^2} \ , \tag{2.2}$$

where d is the waveguide core thickness, n_{core} is the core index of refraction and n_{cladding} is the cladding index of refraction. For such a waveguide, single mode propagation is obtained for $D < \pi$. By optimizing the width and etching depth of a ridge, single lateral mode emission can be obtained with output powers in the watt range [58]. This concept is utilized in chapter 3, while the influence of the etching depth is shown in Appendix A. Note that in the case of gain guiding, the injected current leads to a small temperature increase that causes an index variation between the waveguide and cladding layers, resulting in a (weak) index guiding effect.

Tapered diode lasers combine a ridge waveguide (RW) section with a TPA section. The RW ensures spatial single mode with a narrow beam waist by means of index guiding, while the TPA section utilizes gain guiding to amplify and guide the emitted light. Such devices provide multiple watts of output power with nearly diffraction limited (single mode) spatial characteristics. As mentioned in the motivation section, TPAs will be utilized in the MOPA systems of this work, see chapter 8.

2.4 Power characteristics

The generated photon emission needs to be amplified by stimulated emission in order to compensate all losses occurring within the resonant cavity. In the case of a Fabry Pérot resonator having a gain medium of length L_{gain} in a cavity of length L_{cav}, positioned between two mirrors of reflectivity R_{f} and R_{b}, see Fig. 2.3, the threshold condition is given by [5]

$$\Gamma g_{\text{th}} = \alpha_{\text{i}} + \alpha_{\text{mirror}} = \alpha_i + \frac{1}{2L_{\text{cav}}} \ln\left(\frac{1}{R_{\text{f}} R_{\text{b}}}\right) \ . \tag{2.3}$$

In the above expression, Γg_{th} is the modal gain, given by the product between the threshold material gain g_{th} and the confinement factor Γ. The latter describes the overlap between the optical mode and the active region of the diode laser. α_{mirror} represents the combined photon losses at the diode laser end facets, while α_i describes the internal losses by intrinsic absorption. For a cavity of a certain gain length L_{gain}, the threshold gain can be reduced by either increasing the cavity length L_{cav} or by increasing the reflectivities of the cavity. This being said, increasing the facet reflectivities could lead to catastrophic optical mirror damage (COMD) affecting the performance and lifetime of a laser. Therefore, the front facet is typically made with low reflectivity, in order to reduce the load on the facet due to the out-coupled light.

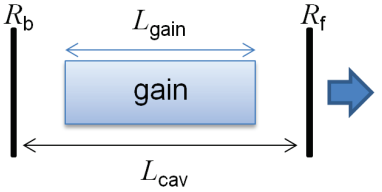

Figure 2.3: *Sketch of a Fabry Pérot resonator.*

After reaching threshold, the output power P shows a linear dependence on the injection current I_{inj} according to [5]

$$P = \eta_i \frac{\alpha_{\text{mirror}}}{\alpha_i + \alpha_{\text{mirror}}} \frac{h\nu}{q} \left(I_{\text{inj}} - I_{\text{th}}\right) = \eta_{\text{d}} \frac{h\nu}{q} \left(I_{\text{inj}} - I_{\text{th}}\right) \ . \tag{2.4}$$

In the above expression, η_i represents the internal efficiency; the fraction of generated photons inside the cavity to the number of carriers, $q = 1.602 \times 10^{-19}$ C is the elementary charge of electrons and I_{th} is threshold current. Finally, η_{d} is the differential efficiency including the internal efficiency and the different losses. This value is defined as

$$\eta_{\mathrm{d}} = \frac{q}{h\nu}\frac{dP}{dI_{\mathrm{inj}}} = \frac{q}{h\nu}S \ , \tag{2.5}$$

where $dP/dI_{\mathrm{inj}} = S$ is the slope efficiency measured in W/A.

The third expression that is typically used to describe lasers is the wall-plug efficiency η_{c}, defined as the ratio between the measured optical power and the injected electrical power:

$$\eta_{\mathrm{c}} = \frac{P}{I_{\mathrm{inj}}V} = \frac{\eta_{\mathrm{d}}\left(I_{\mathrm{inj}} - I_{\mathrm{th}}\right)}{I_{\mathrm{inj}}\left(V_d + I_{\mathrm{inj}}R_{\mathrm{s}}\right)} \ . \tag{2.6}$$

In the above expression, V is the voltage drop of the power supply, V_{d} is the ideal diode voltage (~ 1.2 V for GaAs) and R_{s} is the series resistance. The wall-plug efficiency can be split into four parts:

$$\eta_{\mathrm{c}} = \underbrace{\eta_{\mathrm{i}}}_{1} \ \underbrace{\frac{\alpha_{\mathrm{m}}}{\alpha_{\mathrm{m}} + \alpha_{\mathrm{i}}}}_{2} \ \underbrace{\frac{h\nu}{q\left(V_{\mathrm{d}} + I_{\mathrm{inj}}R_{\mathrm{s}}\right)}}_{3} \ \underbrace{\frac{I_{\mathrm{inj}} - I_{\mathrm{th}}}{I_{\mathrm{inj}}}}_{4} \ , \tag{2.7}$$

which represents:

1. Internal efficiency > 0.9
2. Mirror loss / threshold gain ~ 0.8
3. Electrical loss ~ 0.9 (series resistance)
4. Excess current ~ 0.9

and thus the product of these factors lies between $\eta_{\mathrm{c}} = 0.5$ and 0.6. Although diode lasers exhibits high wall-plug efficiencies, they are typically limited by thermal effects [59, 60]. As the temperature increases in the active region, the carrier confinement decreases and the internal efficiency decreases [5]. By a temperature change of ΔT, the threshold current I_{th} is changed by:

$$I'_{\mathrm{th}} = I_{\mathrm{th}} \exp\left(\frac{\Delta T}{T_0}\right) \ , \tag{2.8}$$

where T_0 is the characteristic temperature of the threshold current. Likewise, the differential efficiency η_{d} is reduced by these thermal effects:

$$\eta'_{\mathrm{d}} = \eta_{\mathrm{d}} \exp\left(\frac{\Delta T}{T_1}\right) \ , \tag{2.9}$$

where T_1 is the characteristic temperature for the above threshold current increment, and is generally two or three times larger than T_0 [52].

These thermal effects are believed to be one of the main reasons behind COMD, which effectively limits the lifetimes of diode lasers [61]. Therefore, heat dissipation of diode lasers is of great importance.

2.5 Spectral properties

The second requirement for lasing is having a resonant optical feedback within the cavity. In the case of a Fabry Pérot resonator of length L_{cav}, standing waves fulfil the requirement:

$$L_{\mathrm{cav}} = \frac{m\lambda_0}{2n_{\mathrm{eff}}} \ , \tag{2.10}$$

with $m = \mathbb{N}$ being the number of the longitudinal modes, λ_0 is the vacuum wavelength and n_{eff} is the effective refractive index of the waveguide inside the laser [5]. In a similar fashion, the mode spacing $\delta\lambda$, often noted as free spectral range (FSR) is given by

$$\delta\lambda = \frac{\lambda_0^2}{2n_{\mathrm{eff}}L_{\mathrm{cav}}} \ . \tag{2.11}$$

In a gain medium close to threshold, only the longitudinal modes closest to the maximum modal gain are amplified. In the case of diode lasers, a gain spectrum wider than $\delta\lambda$ enables spectral multimode emission and subsequently enables wavelength tuning [57].

The emission spectra of diode lasers can be narrowed by different means, e.g. by external or internal gratings. Internally, this is done by using DBR or DFB gratings which provide intrinsic wavelength stabilization. In the latter case, the feedback is distributed throughout the device by introducing periodic perturbations of the refractive index along the length of the active region [62]. In both DBR and DFB gratings, the Bragg condition must be fulfilled:

$$2\Lambda \sin(\theta) = m\lambda_{\mathrm{B}} \ , \tag{2.12}$$

where Λ is the grating period, θ is the angle of incidence, $m = 1, 2, 3, ...$ is the order of the Bragg grating and λ_{B} is the Bragg wavelength [63]. Eq. (2.12) implies that counter propagating waves ($\theta = 90°$) inside the cavity only couple coherently at $\Lambda = m\lambda_{\mathrm{B}}/2$ [57]. Proper engineering of the grating period consequently provides selective feedback, resulting in spectral single-mode emission at λ_{B}.

2.6 Wavelength tuning

When considering wavelength tuning of diode lasers, three parameters should be examined: the optical gain, the feedback and the mode spacing. This is shown in a generic schematic in Fig. 2.4, representing reflectivity and gain versus wavelength. Note that this is a conceptual sketch which is not to scale, as the gain profile is usually 50 to 100 nm broad, with mode spacings of the order of hundreds of picometers, and with sub-picometer wide reflectivity spectrum.

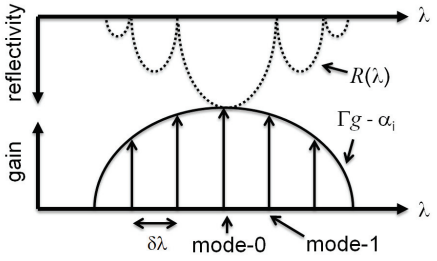

Figure 2.4: *Sketch of the grating reflectivity next to the gain profile including its mode spacing* $\delta\lambda$.

The optical gain in Fig. 2.4 describes the available region of lasing emission and tunability. The shape of the gain profile ($\Gamma g - \alpha_{\mathrm{i}}$) depends on the active medium used for lasing. In the case of quantum well (QW) based diode lasers, the composition and width of the QW structure and the number of embedded QWs determines the gain profile.